Multiscale edge analysis of potential field data

*Nick Archibald
Fractal Graphics Pty Ltd
PO Box 437,
Nedlands, WA, 6009

Paul Gow
CSIRO Division of Exploration and Mining
PO Box 437,
Nedlands, WA, 6009

Fabio Boschetti
CSIRO Division of Exploration and Mining
PO Box 437,
Nedlands, WA, 6009

ABSTRACT

Mapping the three-dimensional distribution of rock properties from potential field data is a difficult and arduous task, with inherent ambiguity remaining a major problem. We apply a combination of automated interpretation procedures, based on multiscale wavelet analysis and three-dimensional visualisation methods, in an attempt to extract geometrical information from potential field datasets, and display this information in an easily understandable and intuitive way. The resulting visualisations are similar to 'worm' maps commonly produced by interpretation of aeromagnetic data, but are defined in three dimensions.

The techniques are tested on a series of synthetic and observed datasets, of varying complexity and geographical scale. The tests show both the effectiveness of the technique as an aid to the geological interpretation of potential field maps and in its use for providing constraints on the three-dimensional geology.

The results of the testing on synthetic datasets show that for certain geometries there is an intuitive relationship between 3D edge location and shape, and subsurface geometries. Such relationships prove particularly robust even under 'noisy' conditions where surface features (e.g. the response of laterites in magnetic datasets) mask the coarser scale features that characterise the broader geological picture.

Three real datasets at different geographical scales have been analysed. These include the Western Australian gravity dataset (representing the continent-scale), aeromagnetic data covering a 1:100,000 scale map sheet from central Victoria (representing the district-scale), and a prospect-scale aeromagnetic dataset from a mineralised greenstone terrane in Western Australia. The results produce different information at the different scales. At the continent-scale the multiscale edges allow

discrimination of different tectonic styles, and comparison of the significance of crustal-scale structures. At the district- to prospect-scale the edges can be used for geological mapping purposes such as to map subtle changes in sedimentary sequences, map alteration patterns, and constrain pluton geometries at depth.

INTRODUCTION

Three dimensional (3D) reconstruction of the subsurface geology is typically a time-consuming process, irrespective of the available constraints. Commonly, analysis of geophysical data is invoked to constrain geometries with depth, typically with a variable degree of automated input. The techniques described below aim to improve the current practices of analysis and 3D geological inversion of potential field data. This is achieved by extracting and visualising in 3D the main features in a potential field map. When viewed in the framework of multiscale wavelet theory, these features have a rigorous relationship to subsurface contacts between zones of different density or magnetic susceptibility, and can thus be employed in an inversion strategy. This kind of inversion has been successfully tested in 2D with synthetic data. Three-dimensional implementation is one of the final aims of this research.

Automated interpretation procedures for potential field data reported in the literature to date have typically focussed on mapping either the depth or rock property contrasts on the surface of the 'magnetic basement'. Examples include analysis of symmetrical and asymmetrical anomaly components by Naudy (1971), the horizontal gradient methods utilised by Cordell & Grauch (1985), and the 3D Euler deconvolution techniques of Reid et al. (1990). Other studies have focussed on mapping the rock property distribution with depth, and include the classic paper from Spector & Grant (1970) and inversion from upward continued data by McGrath

(1991). The techniques reported in this paper can be seen as a generalisation of some of these studies, and work under less restrictive assumptions on the shape of causative sources.

Multiscale edge mapping is a process of mapping edges in potential field data at a variety of spatial scales. On a horizontal plane (ie., in 2D) these edges form individual, isolated 'strings', which are closely related to the lines commonly drawn by geoscientists in 2D visual analysis of potential field maps. When derived in 3D these strings form surfaces (with wavelet scale as the third dimension) whose shape and associated parameters (see the Conceptual Basis section below) are a function of the subsurface 3D location of contacts between bodies of contrasting density and/or magnetic susceptibility. Accordingly such surfaces provide a powerful tool for an insight to the geometries of geological structures at depth.

The process is scale-independent and this paper provides an overview of the way that 3D multiscale edge maps can be used to constrain 3D geological models at a variety of geographical scales. We present several synthetic examples, and data from three studies at different scales. These include:

(i) continent-scale: the gravity map of Western Australia

(ii) district-scale : aeromagnetic data from western-central Victoria

(iii) prospect-scale: aeromagnetic data from the Kambalda Dome area in the Eastern Goldfields of Western Australia.

MULTISCALE ANALYSIS AND POTENTIAL FIELD DATA

Conceptual Basis

The fundamental equations of potential field theory have an interesting interpretation when regarded as a particular case of a multiscale wavelet transform.

Drawing upon recent results in the wavelet processing of images (e.g. Mallat and Zhong, 1992) and of potential fields (e.g. Hornby et al., 1998), we have synthesised new methods of analysing gravity fields, based upon a generalisation of the concept of edges.

Wavelet analysis has been proposed in the last decade in the fields of image processing and applied mathematics, mainly as an alternative to Fourier analysis. A wavelet transform is obtained by convolving a data set with a function (wavelet) that offers better localisation properties than Fourier bases. Many wavelet bases are available and their choice depends on the data and the purpose of the analysis. Hornby et al. (1998) have shown that, with the use of an appropriate wavelet, derived by the Green's function of gravitational acceleration, the measured potential field or its spatial derivatives can be treated as the wavelet transforms of the source distribution, thereby providing a rigorous physical meaning to an apparently abstract mathematical operation. Also, they show that many potential field operations have a very natural and compact expression in wavelet domain. For example, there is an equivalence between potential field upward continuation and change of scale in the wavelet analysis.

Figure 1 helps clarify the overall process. Figure 1a shows the 2-D vertical section of a block-like causative source, with stacked profiles of the gravity response from increasing height above the source (increasing z). In Figure 1b the wavelet transform of the gravity field, from increasing height above the causative source, is shown as a series of stacked horizontal curves. The edges, which correspond to the local maxima of the wavelet transform, are shown as vertical curves in Figure 1b. We term the edges derived from the wavelet transform at a small height above the source as "fine scale", and those from a greater height as "coarse scale". Observe the coincident horizontal location of the boundaries of the source and the fine scale edges.

Figure 1c shows a plot of the absolute value of the wavelet transform maxima, or edge intensity, as a function of the height above the source. The evolution of the intensity of the edges with increasing height (i.e. increasing scale), as well as their location, is uniquely related to the type and location of the causative source. This relation is very robust, even in the presence of significant fine scale edges, thereby obviating the problems brought about by features typically characterised as "high frequency noise". Figure 2 shows the edges for an inclined cylinder, as an example of 3D visualisation. The most obvious feature of this figure is the effect of the cylinder inclination on the shape and location of the edges. If the cylinder was vertical the edges would appear in three-dimensions as a symmetrical cone with the point cut off. Instead, the cone defined by the edges has a central axis inclined towards the plunge direction of the cylinder. We consider this effect of change in the geometry of edges in more detail later in this paper.

The only assumption underlying our interpretation of the edges is that singularities in the mass density distribution of the sources correspond one-to-one with apparent edges in the gravity field. We believe this is a geologically reasonable assumption, and is typically at the core of the standard 'human driven' visual interpretation of magnetic/gravity maps. This also explains why the 3D edges present a very intuitive picture of the potential field to geoscientists.

Apart from their potential for visual interpretation and inversion, the multiscale edges derived from this process can be utilised in other ways. A very important property is that the original image can be reconstructed from the multiscale edges (for details refer to Mallat and Zhong, 1992). As in Fourier analysis, data compression and noise filtering can be undertaken before reconstruction. The important advantage of performing these tasks in the wavelet domain rather than in the Fourier domain is that

they can be implemented as local processes that do not affect the whole dataset. The one-to-one correspondence between features in the map and their edges allows for individual feature enhancement/removal that would not be possible with any other implementation.

There are some potential limitations for this technique of analysis when applied to magnetic data. The wavelet analysis utilises the principles of gravitational acceleration therefore magnetic datasets require processing with a pseudo-gravity transform prior to analysis. This may cause a problem for example if there is considerable remanent magnetisation.

Presentation techniques

Currently, two variables from the multiscale analysis are used for presentation purposes. These are i) the location, and ii) the intensity of the edges. The location of the edges (refer Figure 1b) can be plotted in 3D-space (x-y-z) by utilising the scale of the edges (i.e. degree of upward continuation) as the z-coordinate. The intensity value (refer Figure 1c), which is the absolute value of the wavelet transform maxima at that point, is represented by the colour of the plotted edge using a suitably chosen colour scheme. When the solutions are plotted in 3D space they visually define a surface composed of strings of edges from different z-values, with height representing edges from increasingly upward continued data surfaces. In reality these surfaces are composed of myriad dots, hence the display is computationally intensive requiring powerful computer graphics. In the figures presented below, a 3D relief rendering of the potential field is added beneath the plotted edges. Note that this style of visualisation represents only one example of a vast array of presentation techniques that can be used. We are currently working on other types of visual display such as

skeletonisation of surfaces to allow for greater ease of manipulation.

SYNTHETIC EXAMPLES

Several synthetic examples of multiscale edge analysis are presented below which illustrate the relationship between subsurface geometry and the derived edges. It is clear that the edges are representing rock property contrasts, but some practical examples giving a clear idea of how accurately they are doing this are required. Figure 3 shows the edges detected over the contact of a variably dipping fault, generalised as an infinite slab. The trace of the upper contact of the fault surface is precisely mapped by the edge at z=0, and the dip of the fault is revealed by the direction in which the edge moves with increasing z-value. The relationships between the calculated edges and the fault location and dip direction are exact for this geometry of a slab of large lateral extent. Inversion of the curve to yield the fault geometry proved extremely successful. More complex geometries are still under investigation, however inversion in these cases requires a more general approach and the first steps in that direction are being taken. This synthetic example demonstrates that whilst full inversion is not yet fully implemented, a wealth of very useful semi-quantitative information can be derived from the multiscale edge maps.

The second synthetic example (Fig. 4) is a 3D visualisation of the edges derived from a complex model containing a variety of geometries including sheet-, dyke- and point-style sources. The model has been constructed as a deliberate analogy to common geological geometries. Model elements with different thicknesses, depths, and densities show cross-cutting relationships, and small sources at a variety of depths are superimposed. The 3D edges provide a good representation of the source elements, including sharp mapping of contacts, and, most importantly, delineation of cross-

cutting geometries in such a way as to preserve time superposition. The small scattered random sources have not obscured the responses from the main elements to the extent that where the causative sources have very different shapes (e.g. point- vs. dyke-style), the technique has been able to differentiate both shapes in areas where the geometries are superimposed. Likewise, the changes in colour of the edges at a particular scale reflect sensitive changes in rock-property contrasts across a contact. In this synthetic example there is a distinct colour change in the edges representing the margin of the dyke-style body where it cuts the sheet-style body.

EXAMPLES AT MULTIPLE SCALES

Multiscale edge mapping is being applied to a variety of datasets reflecting very different scales of geology, and yielding results ranging from identifying possible crustal-scale structures to defining the shapes of plutons and mine-scale alteration fronts. We present three examples illustrating the application of multiscale edge mapping to real gravity and magnetic datasets. They illustrate the types and variety of information that can be gained from 3D multiscale edge analysis, and how this can help refine understanding of the geological setting.

Continent scale: Western Australian gravity data

Multiscale edge analysis was performed on a gravity dataset covering Western Australia collected by the Australian Geological Survey Organisation (AGSO). At this large-scale the resulting edges have been useful for several reasons. These include the comparison of tectonic style, definition of terranes and terrane boundaries at different levels in the crust, and delineation of the possible geometries of crustal-scale structures. The gravity dataset and the multiscale edges are shown in Figure 5.

Multiscale edge mapping can provide an empirical-style classification of tectonic-style based on the geometry and density of the edges. The 3D edges produced from the gravity data of Western Australia are used as examples to illustrate this. There is a huge amount of information in this data set and it is beyond the scope of this paper to present a rigourous analysis. However, observations about mobile zones bordering the Archaean cratons illustrate some of the types of information about crustal scale geometry that can be abstracted from the edges. We look at the King Leopold - Halls Creek Orogens (Griffin and Grey, 1990) bordering the Kimberley Block, the Paterson orogen (Clarke, 1991) on the eastern margin of the Pilbara Craton, and the Albany - Fraser Orogen (Nelson et al.,1995) on the south-eastern margin of the Yilgarn Craton.

On the grey-scale image of the gravity data the King Leopold and Halls Creek Orogens appear as a relatively continuous mobile zone on the southern and western margins of the Kimberley Block. This is reflected in the fine scale edges, which, using the arguments presented earlier in this paper, represent shallow crustal features. However, the coarser scale edges, reflecting increasing crustal depth, present a more complex picture. The King Leopold Orogen is no longer dominated by the overall NNW trend reflecting its shallow crustal expression, but by dominant east-west structures which coincide with one direction of transfer faults interpreted by Begg (1987). The more dominant northeast-trending transfer faults which are more commonly interpreted from geophysical and Landsat data (Craig et al.,1984; Drummond et al., 1988) are not readily apparent.

In contrast the Halls Creek Orogen appears far more consistent in orientation. The NNE-trending strike, readily apparent in the grey scale image, is preserved at even the coarsest scale of edges, apparently reflecting the persistence of the orogen to deep crustal levels.

It is fascinating to speculate on the position of the deeper crustal structures in both orogens and the occurrence of kimberlite/lamproite intrusions, particularly as the Argyle diamond pipe is located in the part of the Halls Creek orogen where the interpretation of the edges indicates the greatest depth persistence of the structure.

The Paterson Orogen (Clarke, 1991) on the eastern margin of the Pilbara Craton is readily traceable in the grey scale image beneath Officer Basin sediments and into the Petermann Orogen (Forman and Shaw, 1973) comprising the Musgrave and Arunta Blocks. Equally discernible in the grey scale image is the extension of the Pilbara Craton below the Hamersley Basin. However, with increasingly coarser scale edges a fascinating picture emerges. The edges defining the Musgrave and Arunta complexes remain coherent and the structures dominant at fine scales (i.e. upper crustal features) persist to the coarsest scales calculated in this study. These trends persist below the Officer Basin into the southeastern portion of the Paterson orogen. In contrast, the NNW trend apparent in the very fine scale edges within the Paterson Orogen quickly breaks up at coarse scales and becomes dominated by two significant east-west trending structures; one apparently demarcating the margin of the Pilbara Craton with the Hamersley Basin, and another in the middle of the outcropping portion of the Pilbara Craton. The latter structure must be preserved at crustal levels below the base of the greenstones because there is no evidence of such a structure at the surface.

The gravity signature of the Albany - Fraser Orogen (Nelson et al., 1995) is dominated by the mafic rocks of the Fraser Complex (1300 Ma), both in the grey scale image and the fine scale edges. However within the coarser scale edges the persistence of a structure on the northern margin of the Biranup Complex (cf. Nelson et al., 1995), and coincident with the Jerdacuttup Fault, is strongly evident. The northeastern projection of this structure is coincident with a marked colour change in the edges

reflecting the influence of the Paterson-Petermann orogen trends, and further north again becomes broadly coincident with the Halls Creek Orogen.

Thus multiscale edge visualisation appears to provide a powerful tool to interrogate the 3D geometry of crustal scale structures. Not only does it provide valuable insights into the depth persistence of these structures, but it delineates a significant amount of information about the architecture of tectonic blocks.

District scale: western-central Victoria aeromagnetic data

Multiscale edge analysis was performed on an aeromagnetic dataset from a 1:100,000 scale mapsheet (St. Arnaud) from western-central Victoria (Fig. 6a). The geological terrane consists of a relatively non-magnetic sequence of Palaeozoic slates intruded by a series of high level I-type magnetic granites of the Langi Ghiran Complex, and overlain by Tertiary basalts and gravels (Douglas & Ferguson, 1988).

The resulting edges show information from a variety of scales. The fine-scale edges (Figure 6b) show an almost pervasive magnetic grain. This grain could be attributable to a number of sources, namely:

1. subtle changes in magnetic susceptibility of the sedimentary sequence

2. magnetite/maghemite dispersion associated with sheet-wash

3. dispersed magnetite within basalt flows

A magnetic response is commonly absent on the margins of the strongly magnetic granites. This is possibly due to destruction of magnetite in the thermal aureole, or is a reflection of the lack of maghemite concentration on the steeper slopes surrounding the intrusives which occur as significant topographic highs. The abrupt changes in style (quantity, length and intensity of edges) and/or orientation of the magnetic grain may

reflect changes in structural orientation within the slates, or marked changes in the orientation of drainage patterns or basalt flow directions.

The coarse scale edges (Figure 6c) map the margins of the plutons. Steep sided contacts can be readily discerned from the cupolas. Other outlines map what appear to be drainage patterns of the main deep lead channel. If the analysis had been continued to coarser scales these latter features would disappear quickly leaving only the contacts of the magnetic granites represented in the coarsest scale edges.

Minesite scale: Kambalda Dome

Detailed aeromagnetic data acquired during the mid-1990's over the Kambalda Dome, in the Eastern Goldfields Province of Western Australia, has been analysed using multiscale edge mapping techniques. The area consists of a 15km by 10km portion of a greenstone belt composed of predominantly ultramafic rocks cored by a basalt dome and intruded by high level granites/porphyries (Cowden & Roberts, 1990). The results of the multiscale edge mapping provide insights into the subsurface geometry of the area.

The variable talc-carbonate alteration, and accompanying magnetite destruction, is reflected in the patchy magnetic response (Figure 7). The basal contact of the ultramafic rocks with the underlying basalts is largely evident in the magnetic data and these contacts, where preserved at depth, appear well defined by the coarser scale edges. In certain areas the contact signature is absent in the coarser scale edges, and it is known from drilling results that these areas coincide with granite intrusions. The edge mapping has also clearly defined talc-carbonate alteration fronts, possibly related to through-going structures. The edges also delineate a coherent body west of the core of the dome. This body, which had not been previously recognised, has a

distinctive ovoid geometry (Figure 7) suggestive of a granitoid pluton.

DISCUSSION AND CONCLUSIONS

The examples of 3D multiscale edge analysis presented in this paper, of both synthetic and observed potential field datasets, highlight the way automated interpretation procedures and 3D visualisation techniques can be used to constrain the 3D geometry of areas of complex geology. In particular, the techniques allow us to retrieve detailed semi-quantitative data, and view this data in an intuitive way, that, whilst not a full 3D inversion, can be easily translated to general 3D models of the subsurface geometries. The multiscale edge techniques provide the precise location of rock property contrasts at the surface, but currently only approximate locations at depth. The relationships between edge locations in 3D and source bodies is variable for different geometries. The thin slab model (dipping fault) is well constrained, but other geometries such as blocks, folds, and plugs are still being investigated.

Although multi-scale edge analysis techniques can be readily applied to a range of problems including noise filtering and data compression, current development of the techniques is focussed towards full 3D geological inversion of potential field datasets. Inversion is based on identifying the basic source geometry (point, block, dyke, etc.) from the evolution of intensity and location of the edges with increasing scale, and then inverting using the predicted geometry as a starting point. The next challenge is to combine these new techniques with the known geology to efficiently and routinely produce well constrained subsurface reconstructions.

ACKNOWLEDGMENTS.

Work reported here was conducted as part of the Australian Geodynamic

Cooperative Research Centre (AGCRC) as a collaborative project between the AGCRC, CSIRO Division of Exploration and Mining, and Fractal Graphics. This paper is published with the permission of the Director of the AGCRC. The Australian Geological Survey Organisation, the Geological Survey of Victoria, and Western Mining Corporation Ltd are thanked for permission to use the geophysical data presented in this paper.

REFERENCES

Begg, J., 1987, Structuring and controls on Devonian reef development on the north-west Barbwire and adjacent terranes, Canning basin: APEA Journal, **27**, 137-151.

Clarke, G.L., 1991, Proterozoic tectonic reworking of the Rudall Complex, Western Australia: Austral. J. Earth Sci., **38**, 31-44.

Cordell, L., and Grauch, V.J.S., 1985, Mapping basement magnetization zones from aeromagnetic data in the San Juan basin, New Mexico, in Hinze, W.J., Ed., The utility of regional gravity and magnetic anomaly maps: Soc. Expl. Geophys., 181-197.

Cowden, A., and Roberts, D.E., 1990, Komatiite-hosted nickel sulphide deposits, Kambalda, in Hughes, F.E., Ed., Geology of the mineral deposits of Australia and Papua New Guinea: Austral. Inst. Min. Metall., 567-581

Craig, J., Downey, J.W., Gibbs, A.O., and Russell, J.R., 1984, The application of Landsat imagery in structural interpretation of the Canning Basin, Western Australia, in Purcell, P.G., Ed., The Canning Basin, Western Australia: Proceedings of the Geol. Soc. Austr. and Petr. Expl. Soc. Austr. Symposium, Perth, 57-73.

Douglas, J.G., and Ferguson, J.A., 1988, Geology of Victoria, Geol. Soc. Austral.

Drummond, B.J., Etheridge, M.A., Davies, P.J., and Middleton, M.F., 1988, Half-graben model for the structural evolution of the Fitzroy Trough, Canning Basin and implication for resource exploration: APEA Journal, **28**, 76-96.

Forman, D.J., and Shaw, R.D., 1973, Deformation of the crust and mantle in Central Australia: Bur. Min. Res. Austral. Geol. Geophys. Bull, **144**.

Griffin, T.J. and Grey, K., 1990. King Leopold and Halls Creek orogens: Geol. Surv. West. Austral. Mem. **3**, 232-234.

Hornby, P., Boschetti, F., and Horowitz, F., 1998, Analysis of potential field data in the wavelet domain: Accepted for publication in Geophys. J. Internat.

Mallat, S., and Zhong, S., 1992, Characterisation of signals from multiscale edges: IEEE Trans. on Pattern Recognition and Machine Intelligence, **14**, 710-32.

McGrath, P.H., 1991, Dip and depth extent of density boundaries using horizontal derivatives of upward-continued gravity data: GEOPHYSICS, **56**, 1533-1542.

Naudy, H., 1971, Automatic determination of depth from aeromagnetic profiles: GEOPHYSICS, **36**, 717-722.

Nelson, D.R., Myers, J.S., and Nutman, A.P., 1995, Chronology and evolution of the Middle proterozoic Albany - Fraser Orogen, Western Australia: Austral. J. Earth. Sci., **42**, 481-496.

Reid, A.B., Allsop, J.M., Granser, H., Millett, A.J., and Somerton, I.W., 1990, Magnetic interpretation in three dimensions using Euler deconvolution: GEOPHYSICS, **55**, 80-91.

Spector, A., and Grant, F.S., 1970, Statistical models for interpreting aeromagnetic data: GEOPHYSICS, **35**, 293-302.

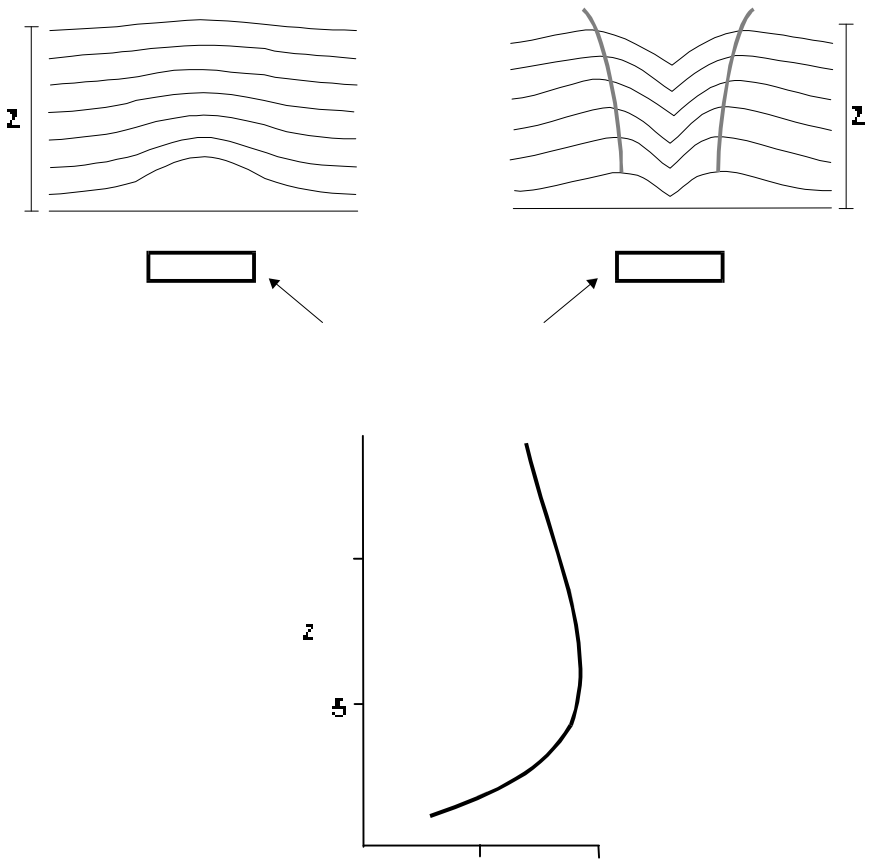

Figure 1: Schematic diagram illustrating the calculation of the intensity of the edges. a) The gravity response over a source body becomes flatter with increasing depth to source (increasing z). b) The absolute value of the wavelet transform is similar to the absolute value of the horizontal gradient. The grey lines on the diagram map the location of the maxima of the wavelet transform. c) The plot of the absolute value of the wavelet transform maxima with increasing height or z-value provides a characteristic curve for different geometries.

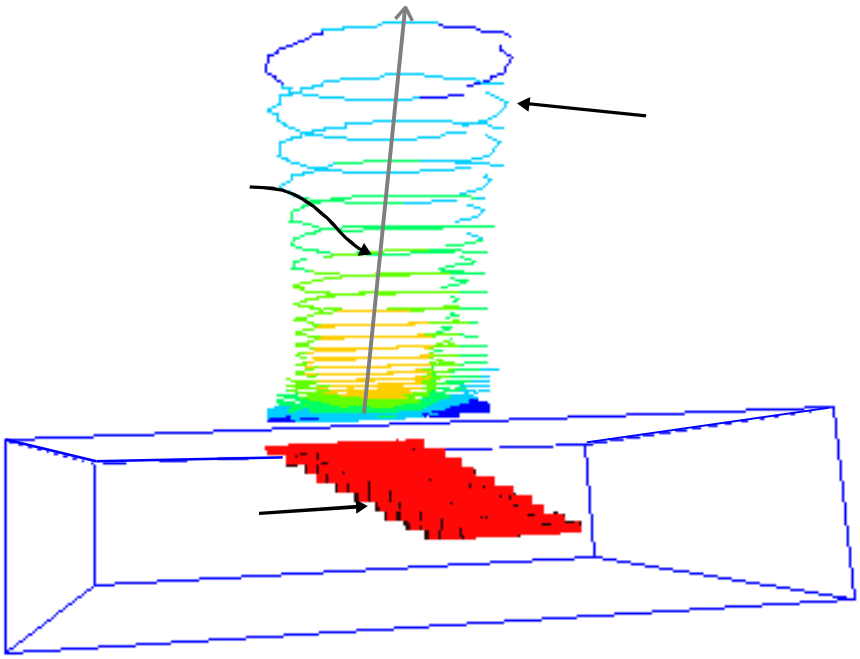

Figure 2: A 3-D visualisation of the multiscale edges due to an inclined cylinder. The edges are plotted with increasing scale upwards. Note the effect of the plunge of the cylinder on the inclination of the axis of the cone formed by the edges.

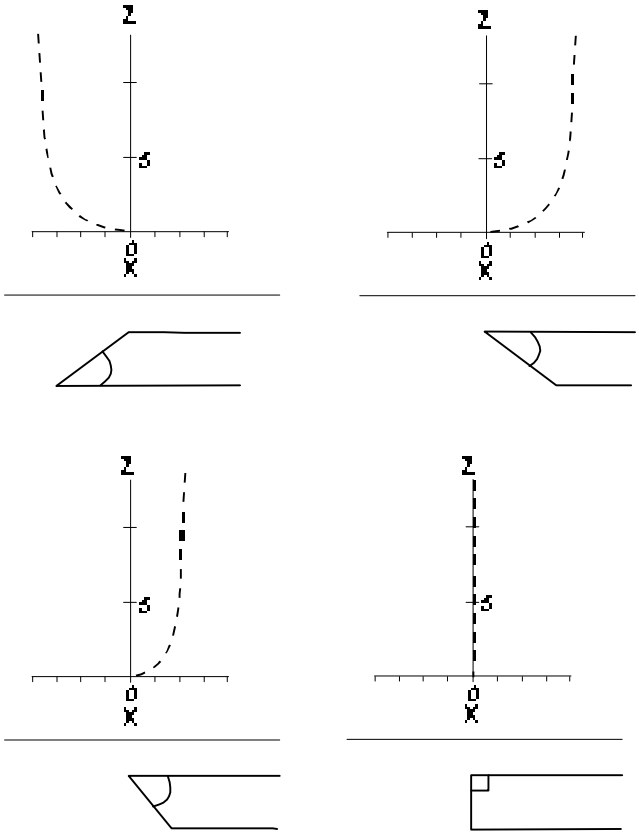

Figure 3: Plots of the wavelet transform maxima over synthetic fault geometries of variable dip (infinite slab model). The z-axis represents the scale of the edges (or the degree of upward continuation), whilst the x-axis is an arbitrary scale showing the position of the edges relative to the fault contact. With increasing scale the edges move in the down-dip direction. Note that the degree of movement of the edges is also dependant on the dip angle of the fault, which allows delineation of relative dip angles.

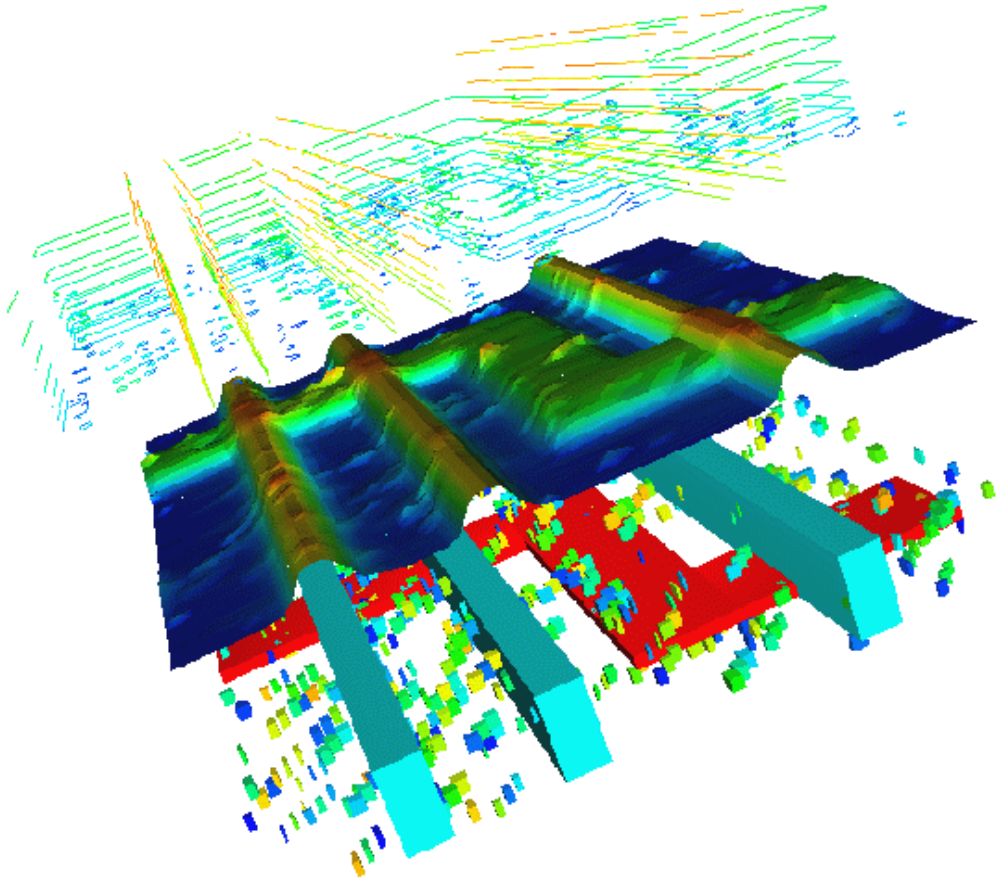

Figure 4: A three-dimensional visualisation of a complex synthetic model and the resulting 3D multiscale edge map. The calculated gravity response is also shown as a pseudocolor image.

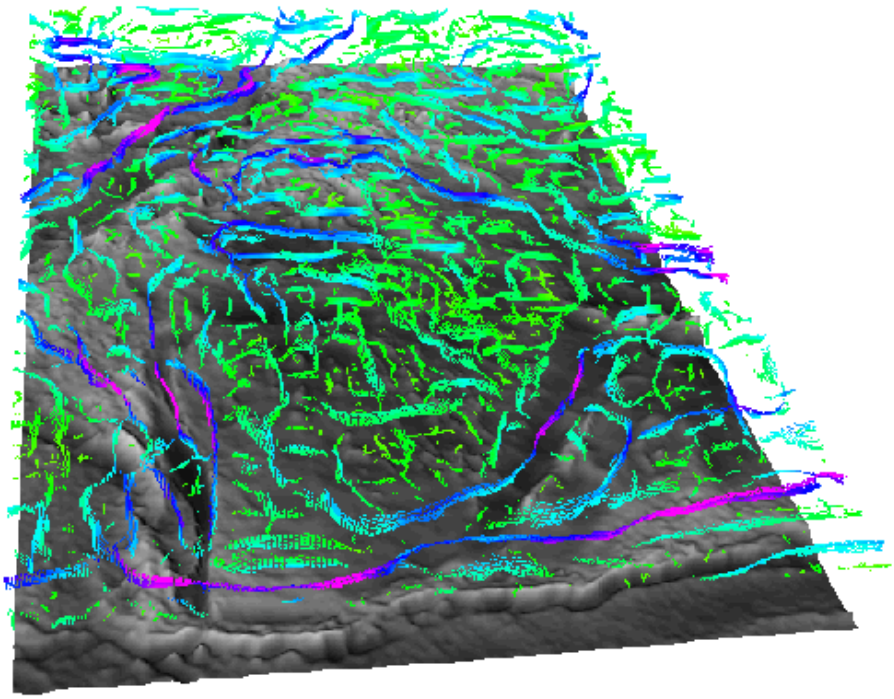

Figure 5: 3D visualisation of the multiscale edge map of the Western Australian gravity data, overlying a relief rendering of the gravity dataset. The view is looking to the north-east.

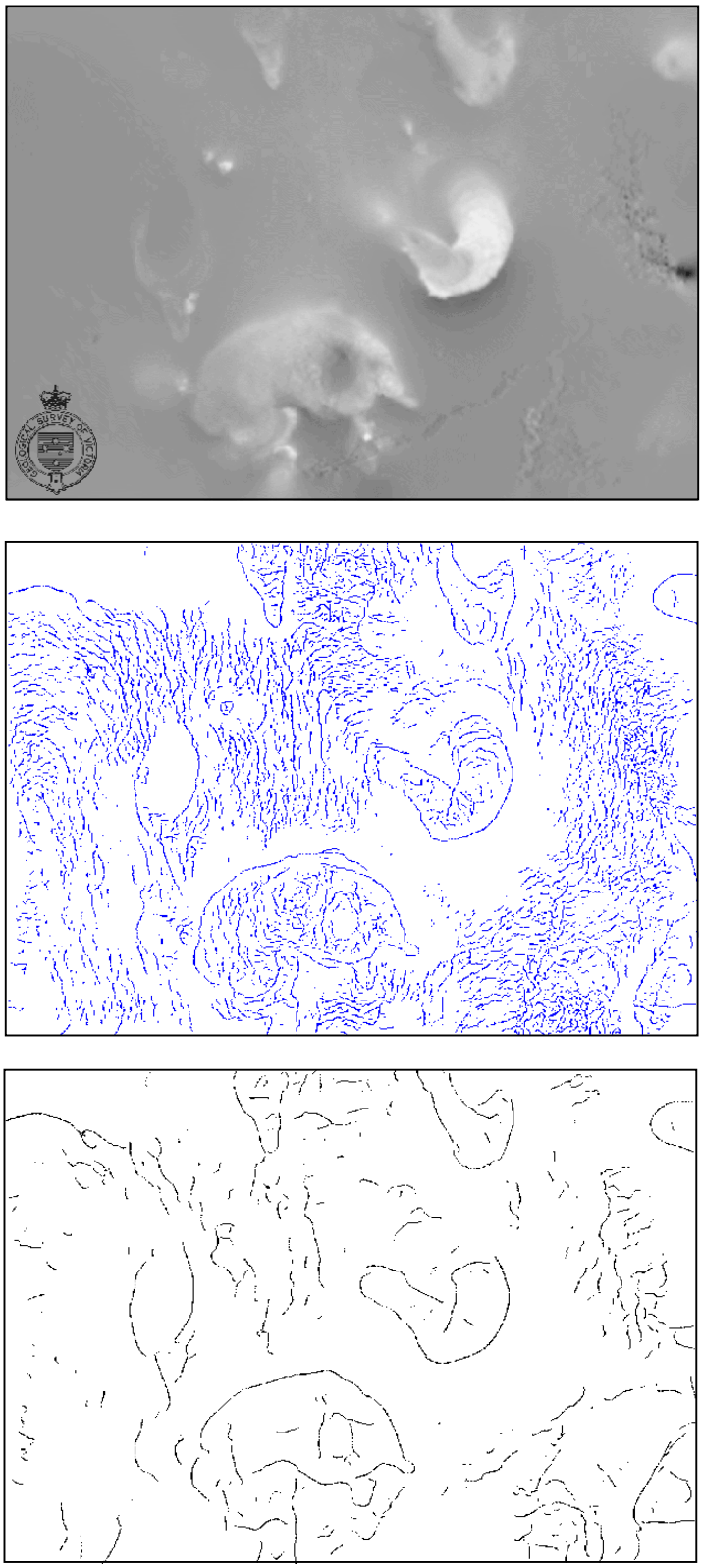

Figure 6: Maps of a) total magnetic intensity and the b) fine scale and c) coarse scale edge maps from the St. Arnaud area in central-western Victoria. The fine-scale data maps subtle variations in the sedimentary sequence, whilst the coarse-scale data maps the granite contacts and drainage patterns.

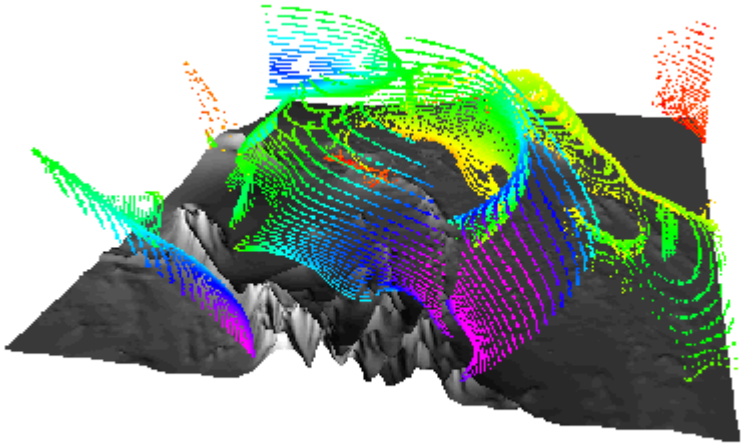

Figure 7: 3D visualisation of the multiscale edge map calculated from detailed aeromagnetic data from the Kambalda Dome area. The image represents the view to the south-west, from north of the dome.